RSC Advances

PAPER

View Article Online
View Journal | View Issue

Cite this: *RSC Adv.*, 2022, **12**, 8674

Iodine(I) complexes incorporating sterically bulky 2-substituted pyridines†

Jas S. Ward, *[a] Rosa M. Gomila, [b] Antonio Frontera [b] and Kari Rissanen [a]

Received 2nd March 2022
Accepted 14th March 2022

DOI: 10.1039/d2ra01390h

rsc.li/rsc-advances

The silver(I) and iodine(I) complexes of the 2-substituted pyridines 2-(diphenylmethyl)pyridine (**1**) and 2-(1,1-diphenylethyl)pyridine (**2**), along with their potential protonated side products, were synthesised to investigate the steric limitations of iodine(I) complex formation. The complexes were characterised by ^{1}H and ^{1}H–^{15}N HMBC NMR, X-ray crystallography, and DFT calculations. The solid-state structures for the silver(I) and iodine(I) complexes were extensively compared to the literature and analysed by DFT to examine the influence of the sterically bulky pyridines and their anions.

Introduction

Since their advent in the 1960s,[1,2] halogen(I) (also known as *halonium*) ions, X^+ (X = Br, I), stabilised by a pair of Lewis bases (L) in the form $[L–X–L]^+$, have existed as examples of halogen group elements formally in the unusual +1 oxidation state, though it was not until the 1990s that they gained mainstream recognition due to the myriad of organic transformations they were deftly demonstrated to effect.[3–5] In addition to this utility, halogen(I) ions possess other favourable properties arising from their σ-hole interaction,[6] most notably the reliable high degree of linear directionality which has been fruitfully utilised in self-assembling supramolecular architectures,[7–9] and recently in coordination polymers such as halogen-bonded organic frameworks (XOFs).[10]

Halogen(I) complexes can be straightforwardly synthesised in a one pot reaction by addition of an elemental halogen, X_2 (X = Br, I) to the analogous 2-coordinate silver(I) complex by Ag^+ to X^+ cation exchange,[11,12,14] or as was recently shown, also from 3-coordinate silver(I) complexes *via* partial cation exchange.[15,16]

The use of substituted pyridines as the stabilising Lewis bases dominates the literature of halogen(I) complexes, and of those examples, it is pyridines substituted in the 4-position which overwhelmingly comprise the largest subset after pyridine itself.[17] The 4-position of coordinating pyridines is one that can be described as only electronically affecting halogen(I) ion formation, and has been previously utilised to explore that relationship in halogen(I) complexes.[11] With respect to the relationship of sterics toward halogen(I) formation, currently the iodine(I) complexes in the literature with the most steric bulk around the I^+ ion are those incorporating 2,6-dimethylpyridine (2,6-lutidine) and 2,4,6-trimethylpyridine,[18–22] as well as a single solid-state example of a bromine(I) complex with quinoline as the Lewis base,[23] though this is not including the molecular clamps reported by Erdélyi and co-workers as those ligands would also provide an additional stabilising contribution *via* the chelate effect.[9,11] Barluenga's reagent, $[I(py)_2]BF_4$ (py = pyridine), the ubiquitous iodination reagent for which iodine(I) chemistry owes its current renown, is commercially available and demonstrates a vast scope of utility, however, decomposition is observed over time. Therefore, an expansion of the pyridine scaffold would be an ideal starting point to explore the steric limitations of halogen(I) ions, and their potential applications toward a new generation of halogen(I) reagents.

Results and discussion

Synthesis and solution studies

The silver(I) complexes [**1**–Ag–**1**]PF_6 (**1a**) and [**2**–Ag–**2**]PF_6 (**2a**) were synthesised quantitatively from the two sterically bulky pyridine-based ligands, 2-(diphenylmethyl)pyridine (**1**) and 2-

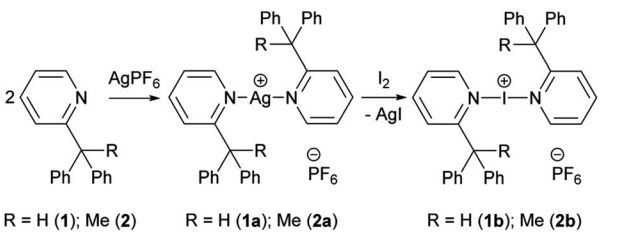

Scheme 1 The synthesis of silver(I) (**1a**, **2a**) and iodine(I) (**1b**, **2b**) complexes of 2-(diphenylmethyl)pyridine (**1**) and 2-(1,1-diphenylethyl)pyridine (**2**).

[a]*University of Jyvaskyla, Department of Chemistry, Jyväskylä 40014, Finland. E-mail: james.s.ward@jyu.fi*

[b]*Department of Chemistry, Universitat de les Illes Balears, Crts de Valldemossa km 7.6, 07122 Palma de Mallorca, Baleares, Spain*

† Electronic supplementary information (ESI) available: Synthesis, NMR, computational details, and X-ray. CCDC 2144042–2144045, 2150094–2150097. For ESI and crystallographic data in CIF or other electronic format see DOI: 10.1039/d2ra01390h

(1,1-diphenylethyl)pyridine (**2**), respectively (Scheme 1). The synthesis of the iodine(I) analogues, [**1**–I–**1**]PF_6 (**1b**) and [**2**–I–**2**]PF_6 (**2b**), were performed by addition of an equivalent of elemental iodine. The reactions were all followed by ^{1}H and ^{1}H–^{15}N correlated NMR spectroscopy.

The ^{1}H NMR spectra of the free ligand **1**, to Ag^+ complex **1a**, and finally to I^+ complex **1b** revealed that all peaks demonstrate noticeable shifts for each transformation, with the ranges of 0.04–0.56 ppm (**1** to **1a**) and 0.01–0.84 ppm (**1a** to **1b**), the most apparent being those for the downfield pyridyl and upfield methine resonances that are free from overlapping chemical shifts with the pendant phenyl rings (Fig. 1). Whilst the ^{1}H NMR data did provide clear indications of clean reactions occurring, they could not themselves point toward the identity of the products. It should be noted that the pyridyl resonances in **1a** (green) do not follow the trend of shifting toward downfield as observed for **1** to **1b**, which is likely due to the increased electron density on the pyridyl rings due to retro-donation with the Ag^+ metal centre.

In contrast, from the ^{1}H–^{15}N HMBC NMR experiments, the ^{15}N NMR chemical shifts of −65.4 ppm (**1**), −118.6 ppm (**1a**), and −165.7 ppm (**1b**) are characteristic of the desired conversions having been achieved, resembling results observed for other iodine(I) complexes of 4-substituted pyridine analogues.[12,13] Anticipating an increased likelihood of decomposition due to the steric hindrance of the substituents in the 2-positions of the pyridyl rings, the protonated (**1c**) and hydronium (**1d**) complexes were deliberately synthesised for comparison, which gave ^{15}N NMR chemical shifts of −167.5 and −122.5 ppm, respectively. Given the reactivity of halogen(I) complexes, their propensity to decompose to protonated species, and the similarity of the ^{15}N NMR chemical shifts of **1a** to **1d** ($\Delta\delta_{15N} = 3.9$ ppm) and **1b** to **1c** ($\Delta\delta_{15N} = 1.8$ ppm), caution must always be taken in characterising halogen(I) species based solely on NMR spectroscopy data. Nevertheless, the identity of **1a** and **1b** were definitely confirmed by single crystal X-ray diffraction studies.

The conversion of the free ligand **2** to the Ag^+ complex **2a** demonstrated similar changes in the ^{1}H NMR chemical shifts as observed for **1** to **1a**, with a range of 0.07–0.90 ppm, and ^{15}N NMR chemical shifts of −65.1 ppm (**2**) and −111.4 ppm (**2a**). However, despite the precipitation of the AgI by-product of cation exchange upon addition of elemental iodine to effect the transformation of **2a** to **2b**, NMR studies suggested that the desired iodine(I) complex **2b** had already begun to decompose within minutes of its inception. The ^{1}H NMR spectrum showed that the pyridyl protons were significantly broadened, and the concomitant ^{1}H–^{15}N HMBC experiment gave a ^{15}N NMR chemical shift of −121.5 ppm.‡ This ^{15}N NMR chemical shift was far from the expected value of approximately −165 ppm for the desired iodine(I) complex **2b**, though it did match well to the independently synthesised hydronium species [**2**–H–**2**]PF_6 (**2d**), which had a ^{15}N NMR chemical shift of −123.0 ppm.

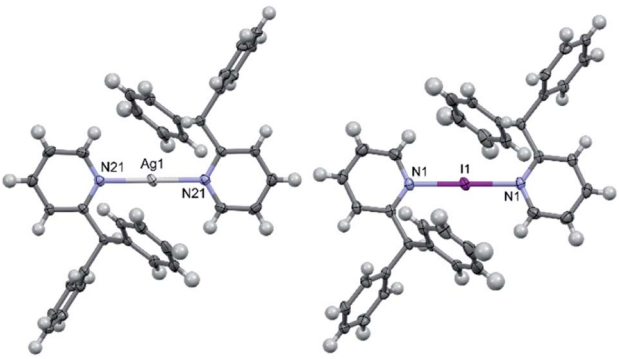

Fig. 2 The X-ray crystal structures of the cations of [**1**–Ag–**1**]PF_6 (**1a**; left) and [**1**–I–**1**]PF_6 (**1b**; right) showing the *anti*-configuration of the ligands due to steric considerations (PF_6 anions omitted for clarity; thermal ellipsoids at 50% probability).

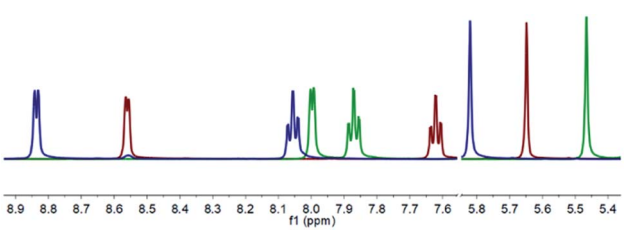

Fig. 1 The superimposed 1H NMR spectra of **1** (red), **1a** (green), and **1b** (blue) of their non-overlapping pyridyl and methine resonances in CD_2Cl_2 (500 MHz, 298 K).

Solid-state studies

The solid-state structure of **1a** contained two half cations which self-completed by symmetry, and similarly **1b** contained just one half, which in both instances ensured that all N–Ag–N and N–I–N angles were symmetry enforced, *i.e.*, perfectly linear. The slightly elongated Ag–N bond lengths of 2.151(2) and 2.162(2) Å in **1a**, in combination with the I–N bond length of 2.273(3) Å in **1b**, were as expected and unremarkable when compared to those observed for [Ag(pyridine)$_2$]PF_6 (2.129(6) Å) and [I(pyridine)$_2$]PF_6 (2.268(2) Å),[24,25] or even the more closely related 2-ethylpyridine (2-Etpy) derivatives [Ag(2-Etpy)$_2$]PF_6 (2.128(3)/2.130(3) Å) and [I(2-Etpy)$_2$]PF_6 (2.270(2) Å),[13] with only the silver(I) comparisons being slightly beyond a 3σ tolerance and therefore crystallographically distinguishable from one another. It should be noted that the previously reported [I(2-Etpy)$_2$]PF_6 adopted a counterintuitive *syn*-configuration of the 2-ethyl substituents, with concomitant loss of co-planarity (an angle of 32.4° between the planes of the two pyridyl rings was found). However, in both **1a** and **1b**, the ligands were co-planar and, as expected, assumed *anti*-configurations (Fig. 2) due to steric considerations, with one of the two pendant phenyl rings pointing directly away from the Ag^+ or I^+ centres, respectively.

Interestingly, the I^+ centre of **1b** is noticeably exerting an increased repulsion on the 2-substituents, despite the ligands being further apart from one another and the I^+ when compared

‡ The ^{1}H NMR spectrum was collected within 5 minutes of I_2 addition, but a satisfactory ^{1}H–^{15}N HMBC experiment took several hours to complete to give the chemical shift stated.

to the Ag^+ in **1a**. This distortion is not readily apparent in the previously discussed bond lengths or angles, but can be quantified by comparison of the $I^+\cdots$pyridyl(C2)/$I^+\cdots$pyridyl(C6) through-space distances in **1b** of 3.074(5)/3.252(4) Å, which are reminiscent of those observed for $[I(2\text{-Etpy})_2]PF_6$ of 3.086(2)/3.244(2) Å, and are clearly deviating from the more alike pair of distances of $Ag^+\cdots$pyridyl(C2)/$Ag^+\cdots$pyridyl(C6) in **1a** of 3.065(2)/3.070(2) Å and 3.050(3)/3.085(2) Å. Whilst a few examples of discrete silver(I) complexes have been reported with similarly sterically bulky 2-substituted pyridines,[17,26] though all less sterically encumbered than **1a** and **2a**, no examples of such sterically endowed iodine(I) complexes currently exist in the literature.

The solid-state structure of **2a** (Fig. 3) revealed significantly lengthened Ag–N bond lengths of 2.210(2) and 2.210(2) Å, which are, as best as can be determined,[17] some of the longest known to date for a discrete, linear silver(I) complex incorporating 2-substituted pyridines, only rivalled by those of $[Ag(4\text{-(phenylethynyl)pyridine})_2]^+$ (2.214(5) and 2.217(5) Å).[27] Whilst longer Ag–N bond lengths are present in the literature, in those instances the elongation can be associated to the complexes exhibiting significantly distorted N–Ag–N angles due to partial coordination from another donor to the silver(I) centre, such as coordination from an anion,[28,29] or from strain caused by the ligand system due to it being dimeric/polymeric in nature,[30] or both.[31] Unlike in **1a** and **1b**, the pyridyl ligands in **2a** are not co-planar, nor do they assume an *anti*-configuration, with a N–Ag–N angle of 173.04(7)° and an angle of 78.4° between the planes of the two pyridyl rings. If the deviation from linearity of the N–I–N angle in **2b** was similar to that observed for **2a**, then this could contribute to the high reactivity of **2b**, given that the largest observed deviation from linearity for an iodine(I) complex is for $[I(2\text{-Etpy})_2]PF_6$ with a N–I–N angle of 173.62(10)°.[13]

Whilst an increase in reactivity for **2b** was anticipated relative to **1b** due to the slightly increased steric bulk of its substituent, the rapid decomposition of **2b** was particularly striking in comparison to the only minimal decomposition that was observed after 8 days for a sample of **1b** kept in solution for the duration. The persistence of **1b** is drastically longer than for many other known iodine(I) complexes incorporating Lewis bases with sterically negligible substituents in the 2-positions, such as 2-ethylpyridine and 1-ethylpiperidine,[14] both of which demonstrated behaviour resembling that of **2b**.§.

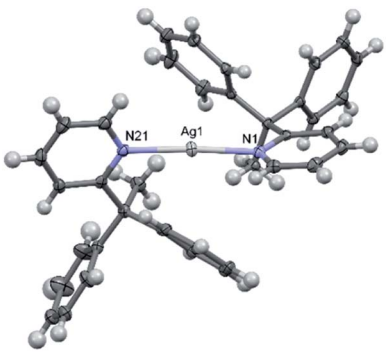

Fig. 3 The X-ray crystal structure of the cation of [**2**–Ag–**2**]PF_6 (**2a**) (PF_6 anion omitted for clarity; thermal ellipsoids at 50% probability).

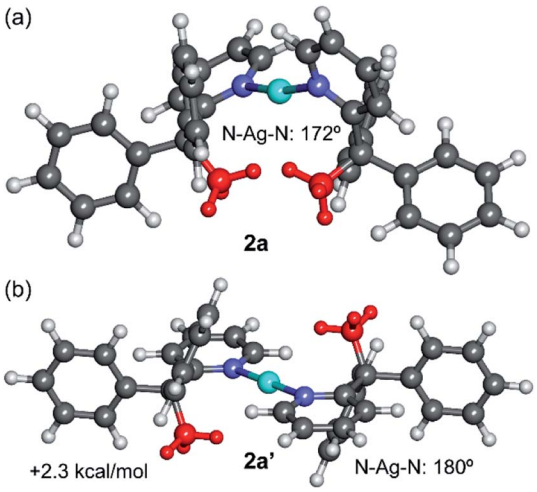

Fig. 4 M06-2X/def2-TZVP optimised geometries of the *syn* (a) and *anti* (b) configurations of the cation of **2a**, with indication of the relative energy. The methyl groups are represented in red.

Computational studies

DFT calculations (M06-2X/def2-TZVP level of theory, see ESI† and theoretical methods below for details) were performed to investigate the counterintuitive *syn*-configuration of **2a** and also to characterise computationally the elusive **2b** structure that could not be structurally characterised by X-ray diffraction methods. Fig. 4 shows the optimised structure of **2a** and the hypothetical *anti*-configuration (denoted as **2a′**), that exhibits a perfectly linear N–Ag–N angle and co-planar pyridyl rings. This configuration is 2.3 kcal mol^{-1} less stable than the *syn*-configuration, in line with the experimental observation.

The DFT optimised structure exhibits a N–Ag–N angle of 172° and angle between the pyridyl rings of 81°, in good agreement with the experimental values (*cf.* 173° and 78°, respectively). Similar agreement, including distances, was observed for the rest of complexes (see ESI, Table S2†), thus giving reliability to this level of theory. The larger stability of the *syn*-configuration in **2a** is most likely due to the contribution of van der Waals interactions between the methyl groups and the aromatic rings, as revealed by the noncovalent interaction plot analysis (NCI-Plot index, see Fig. S43 in the ESI†).

The geometries of the *syn*- and *anti*-configurations of compound **2b** were also calculated (Fig. 5). The calculations reveal that both isomers are practically isoenergetic (the *syn*-configuration is only 0.2 kcal mol^{-1} more stable). A likely explanation is that the stabilisation due to the co-planarity of the rings in the *anti*-configuration is more important in the iodine(I) complex **2b** than in the silver(I) complex **2a**. In fact, the

§ Despite decomposition of $[I(2\text{-Etpy})_2]PF_6$ being observed within minutes of its synthesis by NMR studies, it was robust enough for its solid-state structure to be obtained.[13]

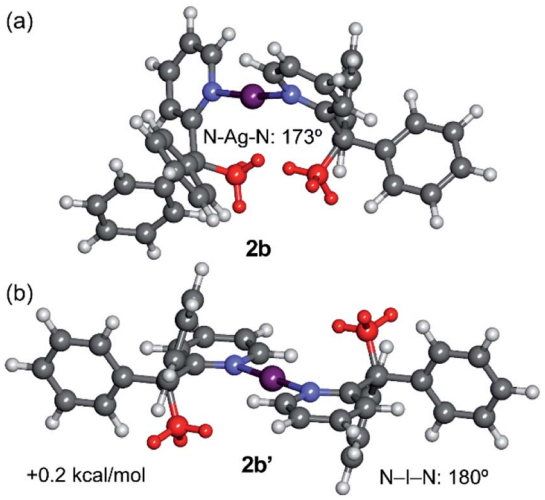

Fig. 5 M06-2X/def2-TZVP optimised geometries of the *syn* (a) and *anti* (b) configurations of the cation of **2b**, with indication of the relative energy. The methyl groups are represented in red.

anti-configuration facilitates the back-donation from the iodine atom (free lone pair) to the π-system, which is important in iodine(I) complexes.[14] This effect compensates for the van der Waals interactions that are established in the *syn*-configuration, which are also less important in **2b**, as revealed by the NCIPlot index (Fig. S43†). The geometries of the Ag^+ and I^+ compounds (**2a** and **2b**) in the *anti*-configuration are very similar. In contrast, those in the *syn*-configuration (**2a′** and **2b′**) are more different, especially regarding the pyridyl ring plane angles that differ by 21° (*cf.* 60° in **2b′** and 81° in **2a′**).

Finally, the dissociation energies (measured as $[L–I–L]^+$ to $I^+ + 2L$; E_{dis}) and I–N distances of the iodine(I) complexes **1b** and **2b** were compared with previously reported examples instead incorporating the quinuclidine (quin) and dimethylaminopyridine (DMAP) ligands (Table 1).[14] The results show the greatest stability for the $[I(quin)_2]^+$ and $[I(DMAP)_2]^+$ complexes followed by **1b** and **2b** in line with the I–N distances that are significantly longer in the latter complexes. The lowest dissociation energy corresponds to compound **2b**, which agrees with its higher reactivity as observed in the NMR experiments.

Anion and packing effects

In halogen(I) chemistry, the BF_4 and PF_6 anions are traditionally used owing to their weakly coordinating nature, which therefore do not complicate the well-established Ag^+ to X^+ (X = Br, I) cation exchange process used to synthesise halogen(I) complexes. In the solid state, both the silver(I) complexes **1a** and **2a** showed meaningful interactions with their respective PF_6 anions, though with **2a** as a discrete ion pair and **1a** as a continuous 1D array of $Ag^+\cdots F–PF_4–F\cdots Ag^+\cdots F–PF_4–F$ contacts (Fig. 6). The closest $Ag^+\cdots F$ distances of 2.918(2)/2.990(2) Å for the two independent molecules in **1a** were below the combined van der Waals radii of for these atoms (Ag + F = 3.19 Å), though are comparable to other previously reported linear silver(I) complexes, such as $[Ag(2\text{-Etpy})_2]PF_6$ and $[Ag(DMAP)_2]PF_6$.[12,13] Similarly, **1a** was able to successfully synthesise **1b** *via* cation exchange, just as has been reported for the aforementioned literature complexes. However, the closest $Ag^+\cdots F$ distance of 2.810(1) Å in **2a** is significantly shorter than those observed in **1a**, and is reminiscent of silver(I) complexes with more strongly coordinating anions, such as those bearing potential oxygen donors like the nitrate anion. The more strongly bound PF_6 anion in **2a** is likely an outcome of the sterically bulky ligands preventing optimal electronic stabilisation for the Ag^+ centre, which was similarly indicated by the long Ag–N bond lengths observed in **2a** (*vide supra*).

With respect to **1b**, similar to **2a**, it also existed as a discrete ion pair. Previous studies have confirmed that iodine(I) ions intrinsically impose a linear 2-coordination sphere, and unlike their silver(I) counterparts, are insensitive to the identity of the anion present.[25] This is apparent in **1b** with a pair of shortest $I^+\cdots F$ distances of 3.618(5), which were reminiscent of those observed in $[I(2\text{-Etpy})_2]PF_6$ (shortest $I^+\cdots F$ distances = 3.693(2) Å),[13] both of which were well over the combined van der Waals radii of these atoms (*cf.* van der Waals radii of I + F = 3.45 Å), indicating that neither were meaningful interactions.

Intrigued by the influence of the anions on the silver(I) precursors, the BF_4, [**1**–Ag–**1**]BF_4 (**1e**) and [**2**–Ag–**2**]BF_4 (**2e**), and OTf, [**1**–Ag–**1**]OTf (**1f**; OTf = triflate) and [**2**–Ag–**2**]OTf (**2f**), anion analogues were also prepared and crystallised so comparisons could be made (Fig. 7). These anions were selected as they are commonly used in the preparation of halogen(I) complexes, so were more relevant than anions such as nitrate, and safer than others such as the perchlorate anion. Both **1e** and **2e** exist as discrete ion pairs with the BF_4 anions, with the shortest $Ag^+\cdots F$

Table 1 Dissociation energies (E_{dis}, kcal mol^{-1}), I–N distances (d, Å) and N–I–N angles (α, °) at the M062X/def2-TZVP level of theory

	1b	**2b**(*syn*)	**2b** (*anti*)	$[I(quin)_2]^+$	$[I(DMAP)_2]^+$
E_{dis}	126.8	119.8	119.6	179.7	181.8
d	2.273	2.305	2.301	2.288	2.245
α	180	173.8	180	180	180

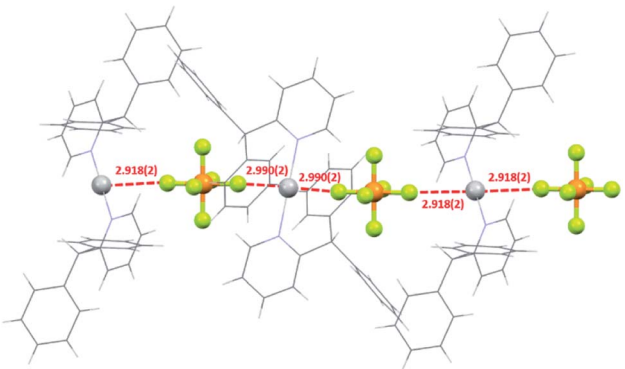

Fig. 6 The packing of three molecules of **1a** showing the 1D network of short Ag^+–F intermolecular interactions (all distances in Å; ligands simplified for clarity).

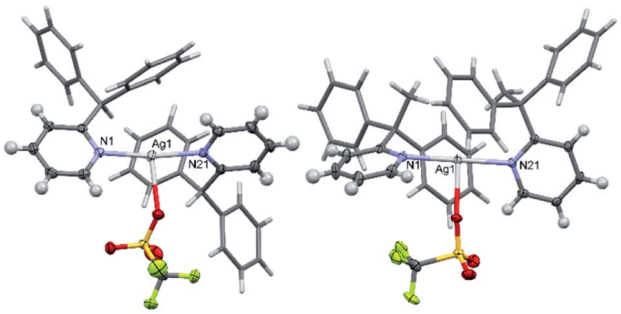

Fig. 7 The X-ray crystal structures of [**1**–Ag–**1**]OTf (**1f**; left) and [**2**–Ag–**2**]OTf (**2f**; right) showing the bound OTf anions (pyridyl substituents simplified for clarity; thermal ellipsoids at 50% probability).

distances of 2.828(5)/2.965(8) Å (the BF_4 anion was found to equally occupy two positions in the solid state) and 2.743(2) Å, respectively. As expected, the OTf anion complexes **1f** and **2f** were observed as neutral T-shaped species, with the OTf anion bound to the Ag^+ centres with Ag^+–O bond lengths of 2.685(2) and 2.578(2) Å, respectively. These matched reported examples of OTf silver(I) complexes incorporating 2-substituted pyridines in the literature, [Ag(2-methoxypyridine)$_2$]OTf and [Ag(2-methylsulfanylpyridine)$_2$]OTf,[32,33] which demonstrated the same T-shaped geometry and similar Ag^+–O bond lengths of 2.679(3) and 2.673(3) Å (minor position (19%) of the disordered OTf anion ignored), respectively.

These solid-state observations were reflected in the solution-state studies of the ^{1}H–^{15}N HMBC determined ^{15}N NMR chemical shifts (Table 2). The values show that the comparisons of the BF_4 (**1e** and **2e**) and PF_6 (**1a** and **2a**) complexes only exhibit negligible differences for the same ligand (**1a** *vs.* **1e** and **2a** *vs.* **2e**), whilst the OTf complexes showed small, but significant, differences of 4.1 (**1a** *vs.* **1f**) and 1.4 (**2a** *vs.* **2f**) ppm when compared to their PF_6 analogues, possibly indicating that the less sterically encumbered complex **1f** continues to interact with the OTf anion in solution, at least more so than **2f**.

A common feature of all silver complexes is that the anion is close to the Ag(I) atom, establishing semi-coordination bonds, or coinage bonds (CiB) according to the nomenclature proposed by some authors.[34,35] These contacts likely influence the Ag–N distance along with the bulkiness of the ligands. The CiBs in complexes **1a, e, f** and **2a, e, f** were analysed using the quantum theory of atoms-in-molecules (QTAIM).[36] Fig. 8 shows the QTAIM representation of the six compounds showing in all cases a bond critical point (CP, represented as red sphere) and bond path (orange line) connecting one atom of the anion to the silver atom, thus confirming the existence of the interaction. In all cases both the Laplacian ($\nabla^2\rho$) of the electron density and the total energy density (H_r) at the bond CP are positive, thus revealing that the Ag···F(O) contacts are noncovalent in nature (CiBs). This is corroborated by the small values or ρ (see Table 3), confirming the weak and closed shell nature of the CiBs. The strength of these CiBs was estimated by using the total energy density at the bond CP and the equation proposed by Espinosa *et al.*[37] This method is convenient to evaluate the noncovalent interaction without the contribution of the pure coulombic attraction between the counterions. These values are indicated in Fig. 8 (annotated in red close to the CPs). The energies range from 2.3 kcal mol^{-1} in **1a** to 9.5 kcal mol^{-1} in **2f**, in line with the Ag···anion distances (see Table 3). It is interesting to highlight that for the complexes with the shortest Ag···anion distance of each series (complexes **1f** and **2f**) the density (ρ, see Table 3) at the bond CP is greater than that in the rest of

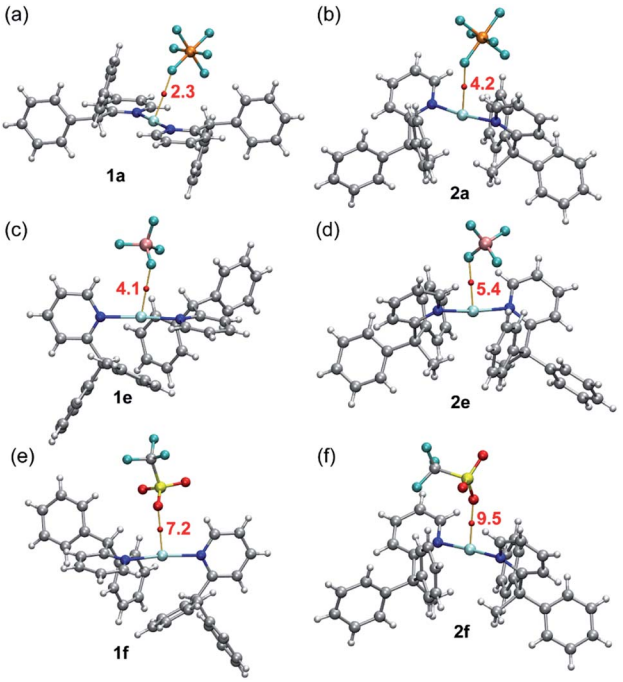

Fig. 8 QTAIM analysis (only the Ag···anion contact is represented for clarity) of compounds **1a** (a), **2a** (b), **1e** (c), **2e** (d), **1f** (e) and **2f** (f). The dissociation energies are indicated in red adjacent to the bond CPs (red spheres).

Table 2 The ^{1}H–^{15}N HMBC determined ^{15}N NMR chemical shifts (ppm) for the silver(I) complexes [**1**–Ag–**1**]$^+$ and [**2**–Ag–**2**]$^+$ with different anions (BF_4, PF_6, and OTf)

Complex	δ_N	Complex	δ_N
[**1**–Ag–**1**]PF_6 (**1a**)	−118.6	[**2**–Ag–**2**]PF_6 (**2a**)	−111.4
[**1**–Ag–**1**]BF_4 (**1e**)	−117.6	[**2**–Ag–**2**]BF_4 (**2e**)	−111.9
[**1**–Ag–**1**]OTf (**1f**)	−114.5	[**2**–Ag–**2**]OTf (**2f**)	−110.0

Table 3 The X-ray Ag–N and Ag···X (X = F, O) distances, density (ρ, a.u.) at the bond CPs represented in Fig. 8 and Wiberg bond indexes (WBI) for all the silver(I) complexes synthesised in this work

Complex	Ag–N	Ag–X	$\rho \times 10^2$	WBI (Ag–N)
1a	2.151	2.990	0.97	0.164 & 0.159
1e	2.150 & 2.155	2.828	1.46	0.144 & 0.150
1f	2.170 & 2.175	2.685	2.23	0.138 & 0.133
2a	2.210	2.818	1.45	0.092 & 0.095
2e	2.215 & 2.219	2.743	1.75	0.081 & 0.091
2f	2.224 & 2.223	2.578	2.67	0.080 & 0.082

complexes, thus suggesting a greater charge transfer from the anion to the Ag(I), thus causing the elongation and weakening of the N–Ag–N bonds, as evidenced by the longer Ag–N distances and smaller Wiberg bond indexes (see Table 3)[38] in complexes **1f** and **2f**.

Conclusions

In conclusion, silver(I) and iodine(I) complexes of sterically bulky 2-substituted pyridines were synthesised and spectroscopically characterised to investigate the steric limitations of iodine(I) ion formation. Three of these complexes, including two silver(I) and one iodine(I) complex, were also definitively confirmed by X-ray diffraction studies, thus demonstrating the possibility to form iodine(I) complexes with sterically bulky ligands in close proximity to the I^+ centre. The effect of the anions on the sterically bulky silver(I) complexes was examined and further explored with a range of different anions, commonly used in halogen(I) chemistry, through extensive DFT studies. DFT calculations were utilised to explain the formation of the *syn*-isomer of **2a**, as well as to study the decreased stability of **2b** with respect to **1b** and other iodine(I) complexes reported in the literature, highlighting the potential of steric control in future halogen(I) chemistry.

Experimental

General considerations

All reagents and solvents were obtained from commercial suppliers and used without further purification, except for 2-(diphenylmethyl)pyridine (**1**) and 2-(1,1-diphenylethyl)pyridine (**2**) which were synthesised according to literature procedures.[39,40] For structural NMR assignments, ^{1}H NMR and ^{1}H–^{15}N NMR correlation spectra were recorded on a Bruker Avance III 500 MHz spectrometer at 25 °C in CD_2Cl_2. Chemical shifts are reported on the δ scale in ppm using the residual solvent signal as internal standard (CH_2Cl_2 in CD_2Cl_2: δ_H 5.32), or for ^{1}H–^{15}N NMR spectroscopy, to an external d_3-$MeNO_2$ standard. For the ^{1}H NMR spectroscopy, each resonance was assigned according to the following conventions: chemical shift (δ) measured in ppm, observed multiplicity, observed coupling constant (J Hz), and number of hydrogen atoms. Multiplicities are denoted as: s (singlet), d (doublet), t (triplet), m (multiplet), and br (broad). For the ^{1}H–^{15}N HMBC spectroscopy, spectral windows of 4 ppm (^{1}H) and 300 ppm (^{15}N) were used, with 1024 points in the direct dimension and 512 increments used in the indirect dimension, with subsequent peak shape analysis being performed to give the reported ^{15}N NMR resonances.

The single crystal X-ray data for **1c** was collected at 120 K using an Agilent SuperNova dual wavelength diffractometer with an Atlas detector using mirror-monochromated Cu-Kα (λ = 1.54184 Å) radiation. The single crystal X-ray data for **1a**, **1b** and **2a** was collected at 120 K using an Agilent SuperNova diffractometer with an Eos detector using mirror-monochromated Mo-Kα (λ = 0.71073 Å) radiation The program CrysAlisPro[41] was used for the data collection and reduction on the SuperNova diffractometer, and the intensities were absorption corrected using a Gaussian face index absorption correction method. All structures were solved by intrinsic phasing (SHELXT)[42] and refined by full-matrix least squares on F^2 using the OLEX2,[43] utilizing the SHELXL-2015 module.[44] Anisotropic displacement parameters were assigned to non-H atoms and isotropic displacement parameters for all H atoms were constrained to multiples of the equivalent displacement parameters of their parent atoms with $U_{iso}(H) = 1.2\ U_{eq}$ (aromatic) or $U_{iso}(H) = 1.5\ U_{eq}$ (alkyl) of their respective parent atoms. The X-ray single crystal data and CCDC numbers of all new structures are included below.

Synthesis and characterisation

All silver(I) and iodine(I) complexes were prepared using the same quantitative general methods, which are given below using [**1**–Ag–**1**]PF_6 (**1a**) and [**1**–I–**1**]PF_6 (**1b**) as examples.

Free ligand 2-(diphenylmethyl)pyridine (1). ^{1}H NMR (500 MHz, CD_2Cl_2) δ 8.56 (d, J = 4.0 Hz, 1H), 7.62 (td, J = 7.7, 1.7 Hz, 1H), 7.30 (t, J = 7.4 Hz, 4H), 7.23 (d, J = 7.3 Hz, 2H), 7.19 (d, J = 7.2 Hz, 4H), 7.17–7.11 (m, 2H), 5.65 (s, 1H); ^{15}N NMR (500 MHz, CD_3CN) δ −65.4. The solid-state structure is known.[45]

Synthesis of [1–Ag–1]PF_6 (1a). A DCM (3 mL) solution of 1 (24.5 mg, 0.1 mmol) was added to $AgPF_6$ (12.6 mg, 0.05 mmol) and the resulting colourless solution stirred for 1.5 hours. All volatiles removed under reduced pressure to leave a white solid. ^{1}H NMR (500 MHz, CD_2Cl_2) δ 8.00 (d, J = 4.5 Hz, 1H), 7.87 (td, J = 7.9, 1.6 Hz, 1H), 7.39–7.33 (m, 7H), 7.17 (d, J = 8.0 Hz, 1H), 7.05 (d, J = 6.7 Hz, 4H), 5.47 (s, 1H); ^{15}N NMR (500 MHz, CD_3CN) δ −118.6. Crystals suitable for single crystal X-ray diffraction were obtained from a DCM solution of **1a** vapour diffused with DIPE. Crystal data for **1a**: CCDC-2144042, $[C_{36}H_{30}AgN_2]PF_6$, M = 743.46, colourless plate, 0.08 × 0.19 × 0.29 mm^3, triclinic, space group $P\bar{1}$ (No. 2), a = 8.5415(3) Å, b = 11.2632(6) Å, c = 16.8492(7) Å, α = 91.301(4)°, β = 97.022(3)°, γ = 101.834(4)°, V = 1572.71(12) Å^3, Z = 2, D_{calc} = 1.570 g cm^{-3}, $F(000)$ = 752, μ = 0.76 mm^{-1}, T = 120.0(1) K, θ_{max} = 29.2°, 7314 total reflections, 5852 with $I_o > 2\sigma(I_o)$, R_{int} = 0.028, 7314 data, 461 parameters, 186 restraints, GooF = 1.06, 0.57 < d$\Delta\rho$ < −0.55 eÅ^{-3}, $R[F^2 > 2\sigma(F^2)]$ = 0.036, $wR(F^2)$ = 0.079.

Synthesis of [1–I–1]PF_6 (1b). A CD_2Cl_2 (0.5 mL) solution of **1** (9.8 mg, 0.04 mmol) was added to $AgPF_6$ (5.1 mg, 0.02 mmol) and the resulting colourless solution stirred for 1.5 hours. I_2 (5.1 mg, 0.02 mmol) was added as a solid and the mixture sonicated for 1 minute to give a red solution and a yellow precipitate, which was used as is for NMR spectroscopic studies. ^{1}H NMR (500 MHz, CD_2Cl_2) δ 8.84 (d, J = 4.8 Hz, 1H), 8.06 (td, J = 7.8, 1.3 Hz, 1H), 7.42–7.31 (m, 7H), 7.23 (d, J = 7.8 Hz, 1H), 6.99 (d, J = 6.6 Hz, 4H), 5.82 (s, 1H); ^{15}N NMR (500 MHz, CD_3CN) δ −165.7. Crystals suitable for single crystal X-ray diffraction were obtained by evaporation of a DCM : pentane (1 : 3) solution of **1b**. Crystal data for **1b**: CCDC-2144043, $[C_{36}H_{30}IN_2]PF_6$, M = 762.49, colourless plate, 0.04 × 0.10 × 0.23 mm^3, monoclinic, space group $C2/c$, a = 20.8912(5) Å, b = 8.1839(2) Å, c = 18.9412(7) Å, β = 94.605(3)°, V = 3227.95(16) Å^3, Z = 4, D_{calc} = 1.569 g cm^{-3}, $F(000)$ = 1528, μ = 1.11 mm^{-1}, T = 120.0(1) K, θ_{max} = 28.0°, 3844 total reflections, 2994 with $I_o > 2\sigma(I_o)$, R_{int} =

0.043, 3844 data, 230 parameters, 51 restraints, GooF = 1.09, 0.74 < dΔρ < −0.75 eÅ^{-3}, $R[F^2 > 2\sigma(F^2)] = 0.046$, $wR(F^2) = 0.100$.

Synthesis of [H(1)]PF_6 (1c). A MeOH (5 mL) solution of **1** (159.4 mg, 0.65 mmol) was diluted with H_2O (1 mL), then conc. HCl (0.1 mL, excess) was added. After 5 minutes of stirring, $[NH_4]PF_6$ (158.9 mg, 0.975 mmol) was added and stirred for a further 5 minutes. The total volume was reduced under reduced pressure to approximately half, at which time a white precipitate was observed. Addition H_2O (7 mL) was added to induce further precipitation, and the white solid collected by filtration (N. B. the dried precipitate was very static prone). Recovered yield = 0.150 mg (0.38 mmol, 59%). ^{1}H NMR (500 MHz, CD_2Cl_2) δ 12.27 (s.br, 1H), 8.37 (d, J = 5.5 Hz, 1H), 8.34 (td, J = 8.0, 1.3 Hz, 1H), 7.77 (t, J = 6.4 Hz, 1H), 7.56 (d, J = 8.1 Hz, 1H), 7.43–7.31 (m, 6H), 7.12 (d, J = 7.0 Hz, 4H), 5.91 (s, 1H); ^{15}N NMR (500 MHz, CD_3CN) δ −167.5. Crystals suitable for single crystal X-ray diffraction were obtained from a DCM solution of **1c** vapour diffused with pentane. Crystal data for **1c**: CCDC-2144044, $[C_{18}H_{16}N]PF_6$, M = 391.29, colourless plate, 0.05 × 0.16 × 0.25 mm^3, monoclinic, space group $P2_1/c$, a = 11.5946(3) Å, b = 19.6879(4) Å, c = 15.0819(4) Å, β = 100.548(2)°, V = 3384.62(14) Å^3, Z = 8, D_{calc} = 1.536 g cm^{-3}, $F(000)$ = 1600, μ = 2.05 mm^{-1}, T = 120.0(1) K, θ_{max} = 76.6°, 6629 total reflections, 5486 with $I_o > 2\sigma(I_o)$, R_{int} = 0.032, 6629 data, 475 parameters, no restraints, GooF = 1.08, 0.66 < dΔρ < −0.25 eÅ^{-3}, $R[F^2 > 2\sigma(F^2)]$ = 0.052, $wR(F^2)$ = 0.145.

Synthesis of [1–H–1]PF_6 (1d). A CD_2Cl_2 (0.5 mL) solution of **1** (4.9 mg, 0.02 mmol) was added to **1c** (7.8 mg, 0.02 mmol), and the resulting colourless solution stirred for 15 minutes before being used for NMR spectroscopic studies. ^{1}H NMR (500 MHz, CD_2Cl_2) δ 8.21 (d, J = 4.4 Hz, 1H), 8.00 (td, J = 7.8, 1.6 Hz, 1H), 7.46 (t, J = 5.7 Hz, 1H), 7.39–7.26 (m, 7H), 7.10 (d, J = 7.1 Hz, 4H), 5.96 (s.br, 0.5H), 5.67 (s, 1H); ^{15}N NMR (500 MHz, CD_3CN) δ −122.5.

Synthesis of [1–Ag–1]BF_4 (1e). Prepared analogously to **1a** using $AgBF_4$ (9.7 mg, 0.05 mmol). ^{1}H NMR (500 MHz, CD_2Cl_2) δ 8.09 (d, J = 4.5 Hz, 2H), 7.85 (td, J = 7.9, 1.5 Hz, 2H), 7.39–7.31 (m, 14H), 7.14 (d, J = 8.0 Hz, 2H), 7.06 (d, J = 7.1 Hz, 8H), 5.51 (s, 2H); ^{15}N NMR (500 MHz, CD_3CN) δ −117.6. Crystals suitable for single crystal X-ray diffraction were obtained from a DCM solution of **1e** vapour diffused with pentane. Crystal data for **1e**: CCDC-2150094, $[C_{36}H_{30}AgN_2]BF_4 \cdot 2(CH_2Cl_2)$, M = 855.15, colourless plate, 0.15 × 0.38 × 0.52 mm^3, monoclinic, space group $P2_1$, a = 9.5033(4) Å, b = 15.3402(6) Å, c = 13.3461(5) Å, β = 108.197(4)°, V = 1848.32(13) Å^3, Z = 2, D_{calc} = 1.537 g cm^{-3}, $F(000)$ = 864, μ = 0.89 mm^{-1}, T = 120.0(1) K, θ_{max} = 27.8°, 7174 total reflections, 6559 with $I_o > 2\sigma(I_o)$, R_{int} = 0.032, 7174 data, 516 parameters, 95 restraints, GooF = 1.08, 0.59 < dΔρ < −0.92 eÅ^{-3}, $R[F^2 > 2\sigma(F^2)]$ = 0.037, $wR(F^2)$ = 0.100.

Synthesis of [1–Ag–1]OTf (1f). Prepared analogously to **1a** using AgOTf (12.8 mg, 0.05 mmol). ^{1}H NMR (500 MHz, CD_2Cl_2) δ 8.17 (d, J = 4.4 Hz, 2H), 7.81 (td, J = 7.8, 1.6 Hz, 2H), 7.38–7.28 (m, 14H), 7.10–7.04 (m, 10H), 5.56 (s, 2H); ^{15}N NMR (500 MHz, CD_3CN) δ −114.5. Crystals suitable for single crystal X-ray diffraction were obtained from a DCM solution of **1f** vapour diffused with Et_2O. Crystal data for **1f**: CCDC-2150095, $[C_{36}H_{30}AgN_2][CF_3O_3S]$, M = 747.56, colourless block, 0.21 × 0.40 × 0.44 mm^3, triclinic, space group $P\bar{1}$ (No. 2), a = 11.3073(5) Å, b = 11.6452(4) Å, c = 15.0627(7) Å, α = 68.117(4)°, β = 85.174(4)°, γ = 71.906(4)°, V = 1748.34(14) Å^3, Z = 2, D_{calc} = 1.420 g cm^{-3}, $F(000)$ = 760, μ = 0.69 mm^{-1}, T = 120.0(1) K, θ_{max} = 29.2°, 8052 total reflections, 6904 with $I_o > 2\sigma(I_o)$, R_{int} = 0.029, 8052 data, 424 parameters, no restraints, GooF = 1.05, 0.44 < dΔρ < −0.54 eÅ^{-3}, $R[F^2 > 2\sigma(F^2)]$ = 0.033, $wR(F^2)$ = 0.077.

Free ligand 2-(1,1-diphenylethyl)pyridine (2). ^{1}H NMR (500 MHz, CD_2Cl_2) δ 8.58 (dt, J = 3.8, 0.8 Hz, 1H), 7.57 (td, J = 7.9, 1.9 Hz, 1H), 7.27 (t, J = 7.4 Hz, 4H), 7.21 (t, J = 7.2 Hz, 2H), 7.15–7.08 (m, 5H), 7.03 (d, J = 8.0 Hz, 1H), 2.20 (s, 3H); ^{15}N NMR (500 MHz, CD_3CN) δ −65.1.

Synthesis of [2–Ag–2]PF_6 (2a). Prepared analogously to **1a** using **2** (25.9 mg, 0.1 mmol). ^{1}H NMR (500 MHz, CD_2Cl_2) δ 7.89 (td, J = 8.1, 1.7 Hz, 1H), 7.68 (d, J = 4.9 Hz, 1H), 7.50 (d, J = 8.1 Hz, 1H), 7.36–7.28 (m, 7H), 7.02 (d, J = 7.0 Hz, 4H), 2.12 (s, 3H); ^{15}N NMR (500 MHz, CD_3CN) δ −111.4. Crystals suitable for single crystal X-ray diffraction were obtained from a DCM solution of **2a** vapour diffused with DIPE. Crystal data for **2a**: CCDC-2144045, $[C_{38}H_{34}AgN_2]PF_6$, M = 771.51, colourless block, 0.13 × 0.20 × 0.37 mm^3, monoclinic, space group $I2/a$, a = 19.5839(3) Å, b = 9.2056(1) Å, c = 36.7734(5) Å, β = 97.273(1)°, V = 6576.23(15) Å^3, Z = 8, D_{calc} = 1.558 g cm^{-3}, $F(000)$ = 3136, μ = 0.73 mm^{-1}, T = 120.0(1) K, θ_{max} = 28.8°, 7810 total reflections, 6708 with $I_o > 2\sigma(I_o)$, R_{int} = 0.030, 7810 data, 435 parameters, no restraints, GooF = 1.04, 0.38 < dΔρ < −0.39 eÅ^{-3}, $R[F^2 > 2\sigma(F^2)]$ = 0.033, $wR(F^2)$ = 0.070.

Attempted synthesis of [2–I–2]PF_6 (2b). Prepared analogously to **1b** using **2** (10.4 mg, 0.04 mmol). ^{1}H NMR (500 MHz, CD_2Cl_2) δ 8.23 (s.br, 1H), 7.96 (td, J = 7.7, 0.9 Hz, 1H), 7.43 (d, J = 7.6 Hz, 2H), 7.36–7.28 (m, 7.0 Hz, 6H), 7.05 (d, J = 7.2 Hz, 4H), 2.22 (s, 3H); ^{15}N NMR (500 MHz, CD_3CN) δ −121.5 (decomposition product).

Synthesis of [H(2)]PF_6 (2c). A MeOH (5 mL) solution of **2** (168.6 mg, 0.65 mmol) was diluted with H_2O (1 mL), then conc. HCl (0.1 mL, excess) was added. After 5 minutes of stirring, $[NH_4]PF_6$ (158.9 mg, 0.975 mmol) was added and stirred for a further 5 minutes. The total volume was reduced under reduced pressure to approximately half, at which time a white precipitate was observed. Addition H_2O (7 mL) was added to induce further precipitation, and the white solid collected by filtration. Product was initially observed as a colourless oil, which solidified after several hours. Recovered yield = 91.6 mg (0.23 mmol, 35%). ^{1}H NMR (500 MHz, CD_2Cl_2) δ 9.12 (s. very br, 1H), 8.74 (dd, J = 5.8, 0.9 Hz, 1H), 8.42 (td, J = 8.1, 1.5 Hz, 1H), 7.86 (dd, J = 6.3, 1.0 Hz, 1H), 7.70 (d, J = 8.2 Hz, 1H), 7.43–7.36 (m, 6H), 7.08 (dd, J = 8.0, 1.3 Hz, 4H), 2.39 (s, 3H); ^{15}N NMR (500 MHz, CD_3CN) δ −180.4.

Synthesis of [2–H–2]PF_6 (2d). A CD_2Cl_2 (0.5 mL) solution of **2** (5.2 mg, 0.02 mmol) was added to **2c** (8.1 mg, 0.02 mmol), and the resulting colourless solution stirred for 15 minutes before being used for NMR spectroscopic studies. ^{1}H NMR (500 MHz, CD_2Cl_2) δ 9.86 (s.br, 0.5H), 8.59 (d, J = 4.4 Hz, 1H), 7.98 (td, J = 8.0, 1.6 Hz, 1H), 7.44 (dd, J = 5.6, 0.8 Hz, 1H), 7.39–7.24 (m, 7H), 7.08 (d, J = 7.2 Hz, 4H), 2.28 (s, 3H); ^{15}N NMR (500 MHz, CD_3CN) δ −123.0.

Synthesis of [2–Ag–2]BF_4 (2e). Prepared analogously to **1a** using **2** (25.9 mg, 0.1 mmol) and $AgBF_4$ (9.7 mg, 0.05 mmol). ^{1}H

NMR (500 MHz, CD_2Cl_2) δ 7.90 (td, J = 8.1, 1.7 Hz, 2H), 7.69 (d, J = 5.0 Hz, 2H), 7.49 (d, J = 8.1 Hz, 2H), 7.37–7.28 (m, 14H), 7.02 (d, J = 7.0 Hz, 8H), 2.12 (s, 6H); ^{15}N NMR (500 MHz, CD_3CN) δ −111.9. Crystals suitable for single crystal X-ray diffraction were obtained from a DCM solution of **2e** vapour diffused with Et_2O. Crystal data for **1a**: CCDC-2150096, $[C_{38}H_{34}AgN_2]BF_4$, M = 713.35, colourless block, 0.21 × 0.38 × 0.50 mm^3, monoclinic, space group $I2/a$, a = 18.1676(3) Å, b = 9.4569(2) Å, c = 37.4652(6) Å, β = 100.690(2)°, V = 6325.2(2) Å^3, Z = 8, D_{calc} = 1.498 g cm^{-3}, $F(000)$ = 2912, μ = 0.69 mm^{-1}, T = 120.0(1) K, θ_{max} = 28.6°, 7397 total reflections, 6250 with $I_o > 2\sigma(I_o)$, R_{int} = 0.043, 7397 data, 417 parameters, no restraints, GooF = 1.04, 0.38 < dΔρ < −0.64 eÅ^{-3}, $R[F^2 > 2\sigma(F^2)]$ = 0.036, $wR(F^2)$ = 0.079.

Synthesis of [2–Ag–2]OTf (2f). Prepared analogously to **1a** using **2** (25.9 mg, 0.1 mmol) and AgOTf (12.8 mg, 0.05 mmol). ^{1}H NMR (500 MHz, CD_2Cl_2) δ 7.86 (td, J = 8.0, 1.7 Hz, 2H), 7.79 (d, J = 4.2 Hz, 2H), 7.42 (d, J = 8.1 Hz, 2H), 7.36–7.26 (m, 14H), 7.04 (d, J = 7.2 Hz, 8H), 2.12 (s, 6H); ^{15}N NMR (500 MHz, CD_3CN) δ −110.0. Crystals suitable for single crystal X-ray diffraction were obtained from a $CHCl_3$ solution of **2f** vapour diffused with pentane. Crystal data for **1a**: CCDC-2150097, $[C_{39}H_{34}AgN_2][CF_3O_3S]$, M = 775.61, colourless plate, 0.06 × 0.07 × 0.32 mm^3, monoclinic, space group $I2/a$, a = 19.7243(4) Å, b = 9.1083(2) Å, c = 37.8599(7) Å, β = 95.788(2)°, V = 6767.0(2) Å^3, Z = 8, D_{calc} = 1.523 g cm^{-3}, $F(000)$ = 3168, μ = 0.72 mm^{-1}, T = 120.0(1) K, θ_{max} = 26.9°, 8076 total reflections, 6092 with $I_o > 2\sigma(I_o)$, R_{int} = 0.063, 8076 data, 451 parameters, 101 restraints, GooF = 1.07, 0.57 < dΔρ < −0.55 eÅ^{-3}, $R[F^2 > 2\sigma(F^2)]$ = 0.046, $wR(F^2)$ = 0.090.

Theoretical methods

For the optimisations and single point calculations the M06-2X[46]/def2-TZVP[47] level of theory and the Turbomole 7.2 program[48] was used. This level of theory was previously used to study similar complexes.[14–16] The def2-TZVP implementation used in this work employs for Ag the ECP-28 set and scalar relativistic effects.[47] Frequency calculations were used to verify that the geometries correspond to true minima on the potential surface (no imaginary frequencies). No symmetry constraints were imposed for the calculations. Solvent calculations were considered using the conductor-like screening model (COSMO).[49] QTAIM and NCIplot index, that is adequate to reveal noncovalent interactions in real space,[50] were computed at the same level of theory by means of the MULTIWFN program[51] and represented using the VMD software.[52] The Wiberg bond index was computed using the NBO 7.0 program[53] at the same level of theory.

Conflicts of interest

There are no conflicts to declare.

Acknowledgements

The authors gratefully acknowledge the Magnus Ehrnrooth Foundation (J. S. W.), the MICIU/AEI of Spain (A. F. project PID2020-115637GB-I00, FEDER), the Academy of Finland (K. R. grant no. 317259), and the University of Jyvaskyla, Finland for financial support.

Notes and references

1 J. A. Creighton, I. Haque and J. L. Wood, *Chem. Commun.*, 1966, 229.
2 I. Haque and J. L. Wood, *J. Mol. Struct.*, 1968, **2**, 217–238.
3 J. Barluenga, J. M. González, M. A. Garcia-Martin, P. J. Campos and G. Asensio, *J. Chem. Soc., Chem. Commun.*, 1992, 1016–1017.
4 J. Ezquerra, C. Pedregal, C. Lamas, J. Barluenga, M. Pérez, M. A. García-Martín and J. M. González, *J. Org. Chem.*, 1996, **61**, 5804–5812.
5 G. Espuña, G. Arsequell, G. Valencia, J. Barluenga, M. Pérez and J. M. González, *Chem. Commun.*, 2000, 1307–1308.
6 J. Pancholi and P. D. Beer, *Coord. Chem. Rev.*, 2020, **416**, 213281.
7 L. Turunen, U. Warzok, R. Puttreddy, N. K. Beyeh, C. A. Schalley and K. Rissanen, *Angew. Chem., Int. Ed.*, 2016, **55**, 14033–14036.
8 L. Turunen, U. Warzok, C. A. Schalley and K. Rissanen, *Chem*, 2017, **3**, 861–869.
9 A. Vanderkooy, A. K. Gupta, T. Földes, S. Lindblad, A. Orthaber, I. Pápai and M. Erdélyi, *Angew. Chem., Int. Ed.*, 2019, **58**, 9012–9016.
10 G. Gong, S. Lv, J. Han, F. Xie, Q. Li, N. Xia, W. Zeng, Y. Chen, L. Wang, J. Wang and S. Chen, *Angew. Chem., Int. Ed.*, 2021, **60**, 14831–14835.
11 A.-C. C. Carlsson, K. Mehmeti, M. Uhrbom, A. Karim, M. Bedin, R. Puttreddy, R. Kleinmaier, A. A. Neverov, B. Nekoueishahraki, J. Gräfenstein, K. Rissanen and M. Erdélyi, *J. Am. Chem. Soc.*, 2016, **138**, 9853–9863.
12 J. S. Ward, G. Fiorini, A. Frontera and K. Rissanen, *Chem. Commun.*, 2020, **56**, 8428–8431.
13 J. S. Ward, A. Frontera and K. Rissanen, *Chem. Commun.*, 2021, **57**, 5094–5097.
14 J. S. Ward, A. Frontera and K. Rissanen, *Dalton Trans.*, 2021, **50**, 8297–8301.
15 S. Yu, P. Kumar, J. S. Ward, A. Frontera and K. Rissanen, *Chem*, 2021, **7**, 948–958.
16 J. S. Ward, A. Frontera and K. Rissanen, *Inorg. Chem.*, 2021, **60**, 5383–5390.
17 C. R. Groom, I. J. Bruno, M. P. Lightfoot and S. C. Ward, *Acta Crystallogr., Sect. B: Struct. Sci., Cryst. Eng. Mater.*, 2016, **72**, 171–179.
18 G. D. Brayer and M. N. G. James, *Acta Crystallogr., Sect. B: Struct. Sci., Cryst. Eng. Mater.*, 1982, **38**, 654–657.
19 A. A. Neverov, H. X. Feng, K. Hamilton and R. S. Brown, *J. Org. Chem.*, 2003, **68**, 3802–3810.
20 A. S. Batsanov, J. A. K. Howard, A. P. Lightfoot, S. J. R. Twiddle and A. Whiting, *Eur. J. Org. Chem.*, 2005, **2005**, 1876–1883.
21 T. Okitsu, S. Yumitate, K. Sato, Y. In and A. Wada, *Chem.–Eur. J.*, 2013, **19**, 4992–4996.

22 L. C. F. Morgan, Y. Kim, J. N. Blandy, C. A. Murray, K. E. Christensen and A. L. Thompson, *Chem. Commun.*, 2018, **54**, 9849–9852.
23 N. W. Alcock and G. B. Robertson, *J. Chem. Soc., Dalton Trans.*, 1975, 2483–2486.
24 C. Y. Chen, J. Y. Zeng and H. M. Lee, *Inorg. Chim. Acta*, 2007, **360**, 21–30.
25 M. Bedin, A. Karim, M. Reitti, A.-C. C. Carlsson, F. Topić, M. Cetina, F. Pan, V. Havel, F. Al-Ameri, V. Sindelar, K. Rissanen, J. Gräfenstein and M. Erdélyi, *Chem. Sci.*, 2015, **6**, 3746–3756.
26 C.-Q. Wan, Q.-S. Li, H.-B. Song, F.-B. Xu and Z.-Z. Zhang, *Acta Crystallogr., Sect. E: Struct. Rep. Online*, 2004, **60**, m1973–m1975.
27 J. V Knichal, W. J. Gee, C. A. Cameron, J. M. Skelton, K. J. Gagnon, S. J. Teat, C. C. Wilson, P. R. Raithby and A. D. Burrows, *Eur. J. Inorg. Chem.*, 2017, **2017**, 1855–1867.
28 M. A. M. Abu-Youssef, R. Dey, Y. Gohar, A. A. Massoud, L. Öhrström and V. Langer, *Inorg. Chem.*, 2007, **46**, 5893–5903.
29 B. Kilduff, D. Pogozhev, S. A. Baudron and M. W. Hosseini, *Inorg. Chem.*, 2010, **49**, 11231–11239.
30 Z. Qin, L. Zhao, Z. Li, S. Tian, Q. Xiao, Y. Deng, J. Zhang, G. Li and C. Wan, *Dalton Trans.*, 2019, **48**, 6730–6737.
31 X.-D. Chen and T. C. W. Mak, *Chem. Commun.*, 2005, 3529–3531.
32 C. Di Nicola, Effendy, F. Marchetti, C. Nervi, C. Pettinari, W. T. Robinson, A. N. Sobolev and A. H. White, *Dalton Trans.*, 2010, **39**, 908–922.
33 M. I. Rogovoy, T. S. Frolova, D. G. Samsonenko, A. S. Berezin, I. Y. Bagryanskaya, N. A. Nedolya, O. A. Tarasova, V. P. Fedin and A. V Artem'ev, *Eur. J. Inorg. Chem.*, 2020, **2020**, 1635–1644.
34 A. C. Legon and N. R. Walker, *Phys. Chem. Chem. Phys.*, 2018, **20**, 19332–19338.
35 A. Daolio, A. Pizzi, G. Terraneo, M. Ursini, A. Frontera and G. Resnati, *Angew. Chem., Int. Ed.*, 2021, **60**, 14385–14389.
36 R. F. W. Bader, *Chem. Rev.*, 1991, **91**, 893–928.
37 E. Espinosa, E. Molins and C. Lecomte, *Chem. Phys. Lett.*, 1998, **285**, 170–173.
38 K. B. Wiberg, *Tetrahedron*, 1968, **24**, 1083–1096.
39 D. A. Klumpp, M. Garza, G. V. Sanchez, S. Lau and S. de Leon, *J. Org. Chem.*, 2000, **65**, 8997–9000.
40 X. Ji, T. Huang, W. Wu, F. Liang and S. Cao, *Org. Lett.*, 2015, **17**, 5096–5099.
41 *CrysAlis Pro*, Agilent Technologies Ltd, 2014.
42 G. M. Sheldrick, *Acta Crystallogr., Sect. A: Found. Adv.*, 2015, **71**, 3–8.
43 O. V. Dolomanov, L. J. Bourhis, R. J. Gildea, J. A. K. Howard and H. Puschmann, *J. Appl. Crystallogr.*, 2009, **42**, 339–341.
44 G. M. Sheldrick, *Acta Crystallogr., Sect. C: Struct. Chem.*, 2015, **71**, 3–8.
45 U. Pieper and D. Stalke, *Organometallics*, 1993, **12**, 1201–1206.
46 Y. Zhao and D. G. Truhlar, *Theor. Chem. Acc.*, 2008, **120**, 215–241.
47 F. Weigend and R. Ahlrichs, *Phys. Chem. Chem. Phys.*, 2005, **7**, 3297–3305.
48 R. Ahlrichs, M. Bär, M. Häser, H. Horn and C. Kölmel, *Chem. Phys. Lett.*, 1989, **162**, 165–169.
49 A. Klamt, *J. Phys. Chem.*, 1995, **99**, 2224–2235.
50 J. Contreras-García, E. R. Johnson, S. Keinan, R. Chaudret, J.-P. Piquemal, D. N. Beratan and W. Yang, *J. Chem. Theory Comput.*, 2011, **7**, 625–632.
51 T. Lu and F. Chen, *J. Comput. Chem.*, 2012, **33**, 580–592.
52 W. Humphrey, A. Dalke and K. Schulten, *J. Mol. Graphics*, 1996, **14**, 33–38.
53 E. D. Glendening, K. Badenhoop, J. A. E. Reed, J. E. Carpenter, J. A. Bohmann, C. M. Morales, P. Karafiloglou, C. R. Landis and F. Weinhold, *NBO 7.0*, 2018.